Supporting Information

Lanthanide f^7 metalloxenes – a class of intrinsic 2D ferromagnets

Andrey M. Tokmachev, Dmitry V. Averyanov, Alexander N. Taldenkov, Oleg E. Parfenov, Igor A. Karateev, Ivan S. Sokolov, Vyacheslav G. Storchak

National Research Center "Kurchatov Institute", Kurchatov Sq. 1, Moscow 123182, Russia

Contents:

Experimental methods

a. Synthesis

$LnGe_2$ (Ln = Eu or Gd) structures are synthesized in the Riber Compact 12 system for molecular beam epitaxy (MBE) furnished with an ultra-high vacuum system. Base pressure in the growth chamber does not exceed 10^{-10} Torr. Direct reaction between Ln and Ge results in $LnGe_2$ compounds. Ge(111) wafers serve both as a reactant and a supporting substrate. As-grown samples are squares with a lateral size of 1 inch. A miscut angle of the wafers is less than 0.5°. To form $LnGe_2$, 4N Eu and 4N Gd are supplied from Knudsen cell effusion sources heated to 400 °C and 1210 °C, respectively. It corresponds to P_{Eu}=$1\cdot10^{-8}$ Torr and P_{Gd}=$1.5\cdot10^{-8}$ Torr, according to a Bayard–Alpert ionization gauge placed at the substrate position. Synthesis of $EuGe_2$ and $GdGe_2$ requires different substrate temperatures: $EuGe_2$ is synthesized at 290 °C, followed by annealing at 500 °C while $GdGe_2$ is produced at 400 °C. Finally, the $LnGe_2$ films are capped at room temperature with a 20 nm layer of insulating SiO_x, to avoid their degradation by air.

b. Structural characterization

The atomic structure of the films is determined by a combination of *in situ* and *ex situ* measurements. In the growth chamber, the film surface is controlled with a reflection high-energy electron diffractometer (RHEED) fitted with the kSA 400 Analytical RHEED system. θ-2θ X-ray diffraction (XRD) scans are produced *ex situ* with the Rigaku Smartlab 9 kW diffractometer employing $CuK_{\alpha1}$ radiation; the lattice parameters c are determined from analysis of all $(000n)$ peaks. The structure is further analyzed with high-resolution electron microscopy. Cross-sections of the films are prepared in the Helios NanoLab 600i scanning electron microscope/focused ion beam (FIB) dual beam system: the sample surface is covered with a 2 μm Pt layer; then, FIB milling with 30 keV Ga^+ ions produces cross-sections measuring 2 μm × 5 μm × 5 μm, which are further thinned and cleaned with 5 keV and 2 keV Ga^+ ions, respectively. Specimens for the top view are also made by FIB using Ga^+ ions. The atomic structure is studied with the TEM/STEM Titan 80-300 microscope employing high-angle annular dark-field (HAADF) imaging. The data are processed with the Digital Micrograph and Tecnai Imaging and Analysis software.

c. Magnetism and electron transport

Data on magnetism of $LnGe_2$ are acquired with the MPMS XL-7 Superconducting Quantum Interference Device (SQUID). The samples (5 mm × 5 mm squares) are mounted in plastic straws; the accuracy of the film orientation with respect to the applied magnetic field is better than 2°. The magnetization is measured employing the reciprocating sample option (RSO). The AFM moments in bulk films are determined by subtracting the diamagnetic moment of the Ge substrate (measured separately) and the paramagnetic contribution modelled by the Brillouin function $cB_{7/2}$ (the same for different directions of the magnetic field, making $\chi(T)$ for $H \| Ge[111]$ approximately a constant below the Néel temperature T_N). Around T_N of

$LnGe_2$, the Ge substrate susceptibility is virtually constant; thus, the subtraction does not influence the shape of the $M(T)$ curves.

An alternative procedure is employed for the FM moments – subtraction of contributions linear in magnetic field. The first step is to measure the magnetic moment χH^* at some high field H^*, so that the FM contribution is small while the other contributions are far from saturation. Then, the FM moment is determined as

$$M_{FM}(H) = M(H) - \chi H.$$

The latter procedure and the former approach – explicit subtraction of the Ge substrate background – produce similar results. It should be noticed that the remnant moment and the difference between FC and ZFC curves do not require any subtraction. Also, the FM moments are detected already in very low magnetic fields where the subtracted contribution is an order of magnitude smaller than the FM moment itself.

The resistivity and Hall effect in the $LnGe_2$ samples are studied with the Lake Shore 9709 A measurement system. The experiments are carried out on square samples 5 mm × 5 mm employing the standard van der Pauw configuration with ohmic contacts made by deposition of an Ag-Sn-Ga alloy on each terminal.

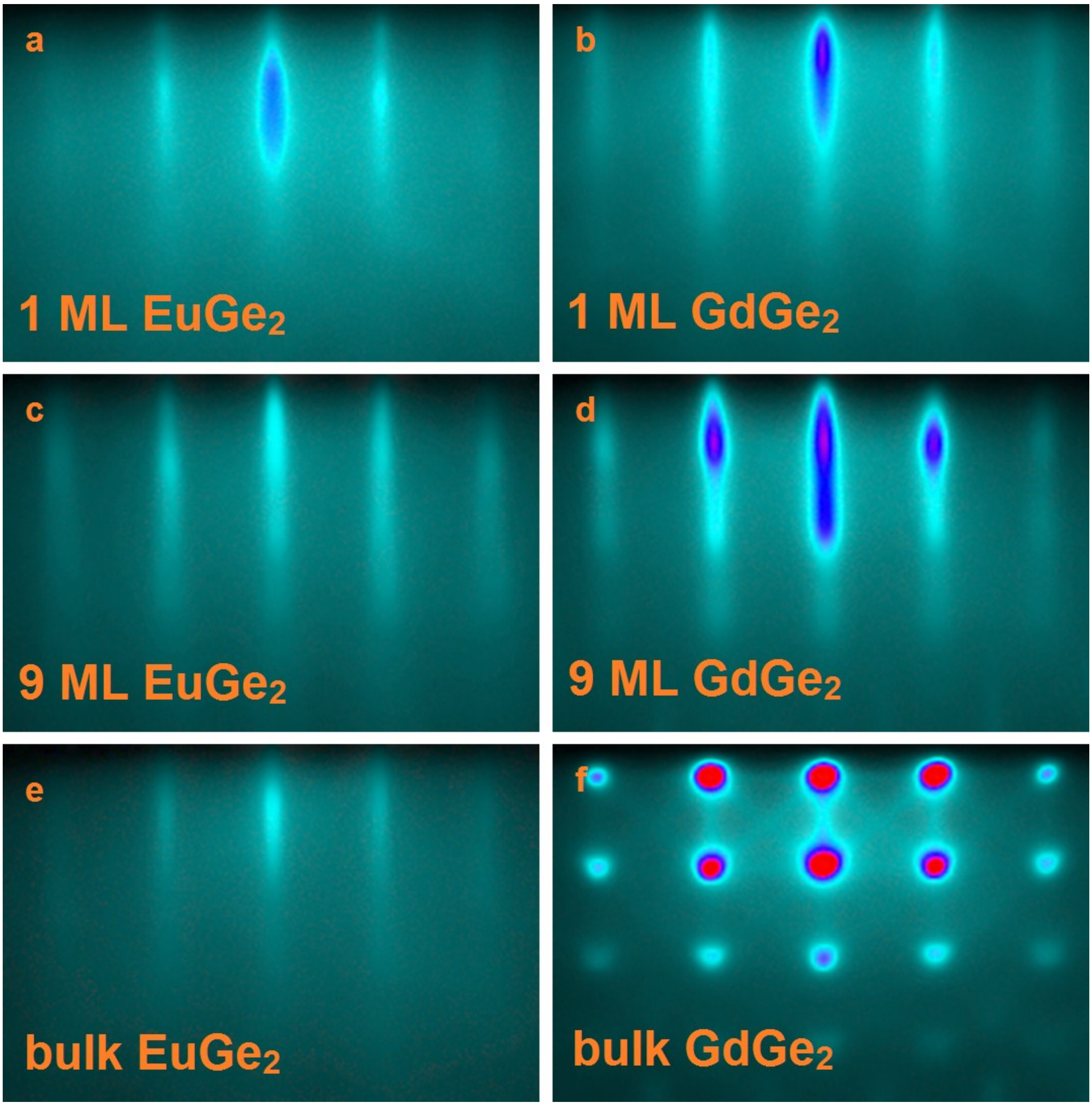

Fig. S1. RHEED images for sequential stages of the $LnGe_2$ film formation. The images are recorded *in situ* and correspond to the $[1\bar{1}0]$ azimuth of the Ge substrate. (a) 1 ML of $EuGe_2$. (b) 1 ML of $GdGe_2$. (c) 9 ML of $EuGe_2$. (d) 9 ML of $GdGe_2$. (e) Bulk $EuGe_2$ (34 nm). (f) Bulk $GdGe_2$ (94 nm).

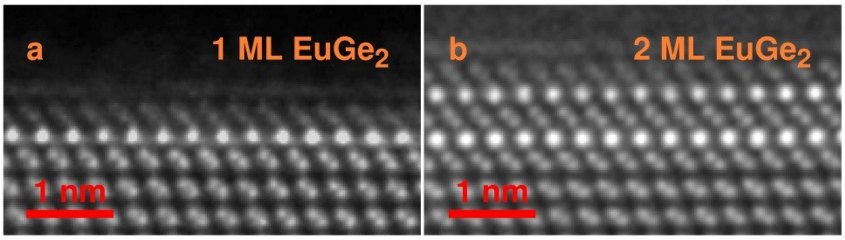

Fig. S2. HAADF-STEM images of $EuGe_2$ on Ge(111) viewed along the $[1\bar{1}0]$ zone axis of the Ge substrate. (a) 1 ML $EuGe_2$. (b) 2 ML $EuGe_2$.

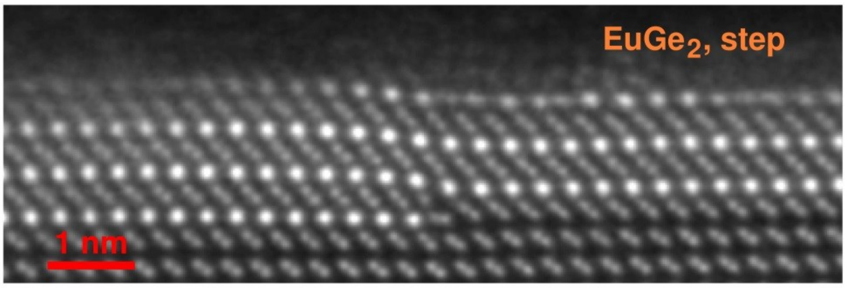

Fig. S3. A HAADF-STEM image of an atomic step in a $EuGe_2$ film arising from terraces on the surface of the Ge(111) substrate. The image is viewed along the $[1\bar{1}0]$ zone axis of the substrate.

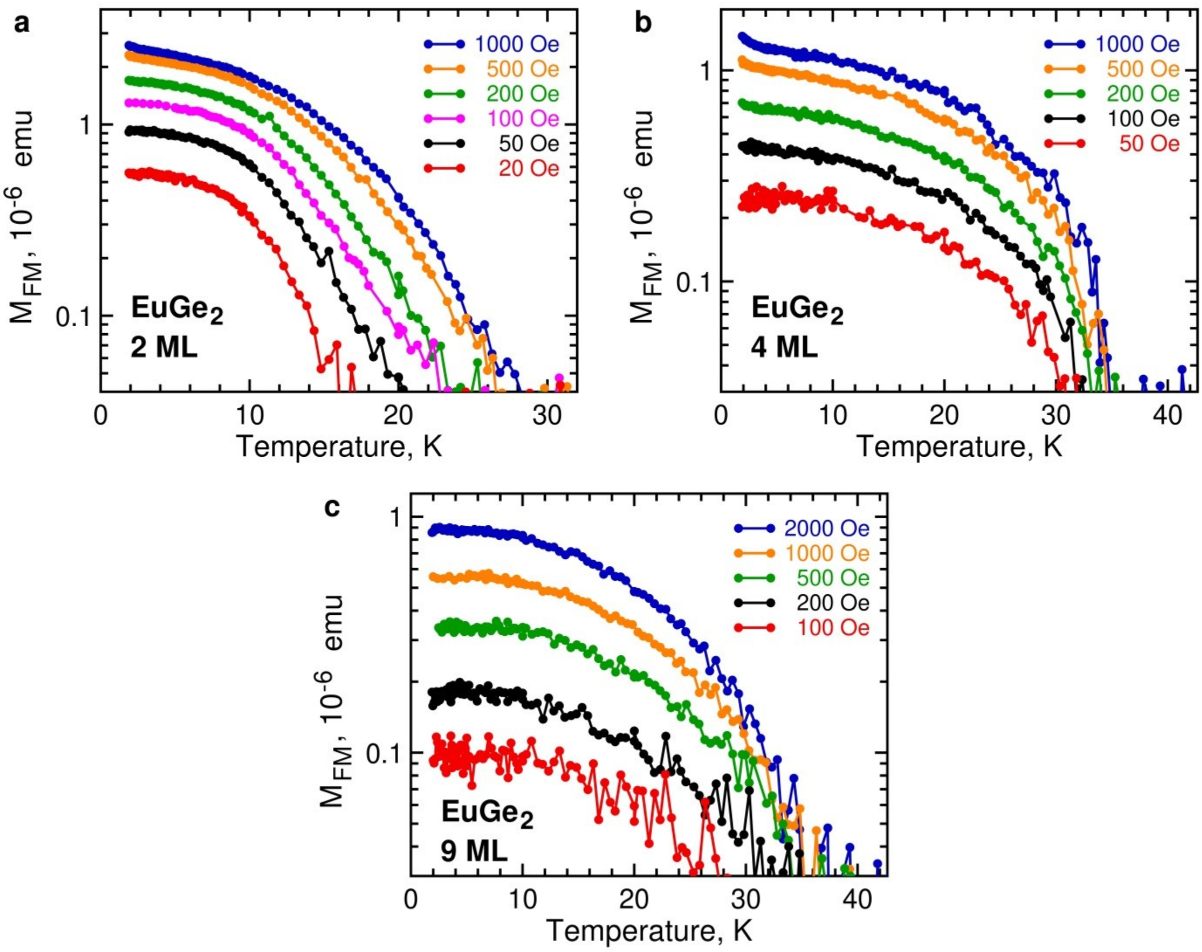

Fig. S4. Temperature dependence of the FM moment measured in a number of magnetic fields along the Ge$[11\bar{2}]$ direction. (a) 2 ML $EuGe_2$. (b) 4 ML $EuGe_2$. (c) 9 ML $EuGe_2$.

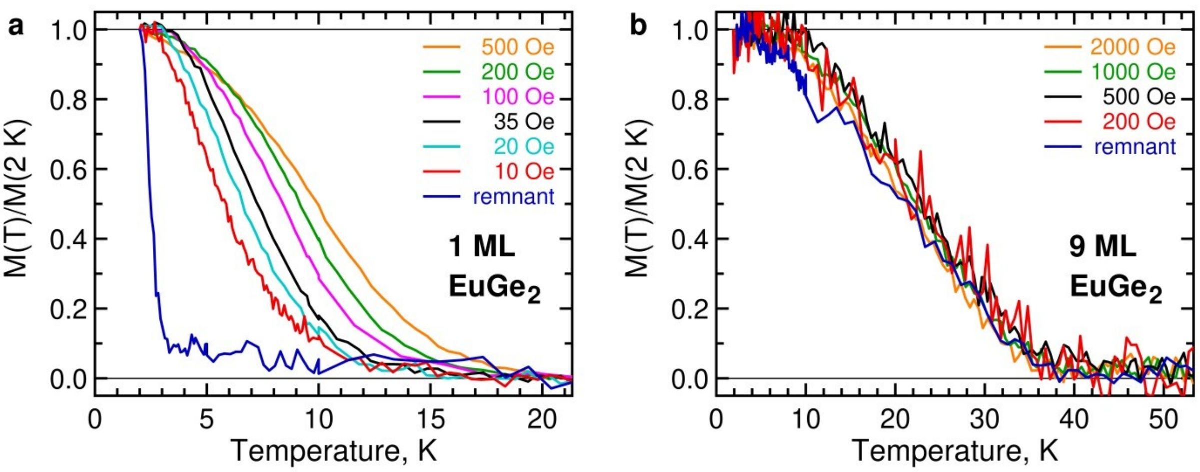

Fig. S5. Temperature dependence of the normalized FM moment measured in a number of magnetic fields along the Ge$[11\bar{2}]$ direction. (a) 1 ML $EuGe_2$. (b) 9 ML $EuGe_2$.

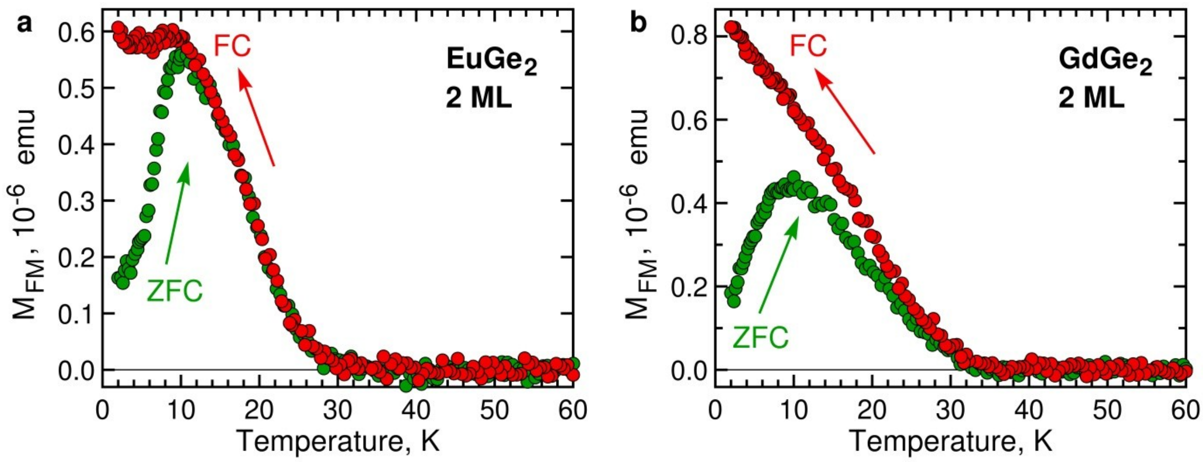

Fig. S6. Zero-field-cooled (ZFC) and field-cooled (FC) magnetization curves for (a) 2 ML $EuGe_2$ (50 Oe) and (b) 2 ML $GdGe_2$ (70 Oe).

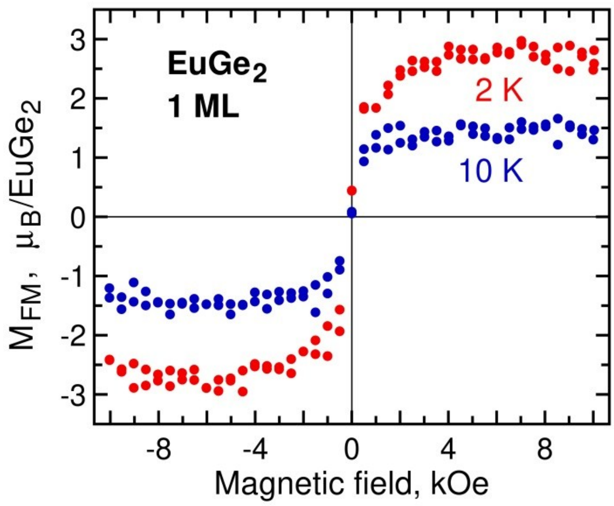

Fig. S7. Magnetic field dependence of the FM moment along the Ge$[11\bar{2}]$ direction in 1 ML $EuGe_2$ on Ge(111).

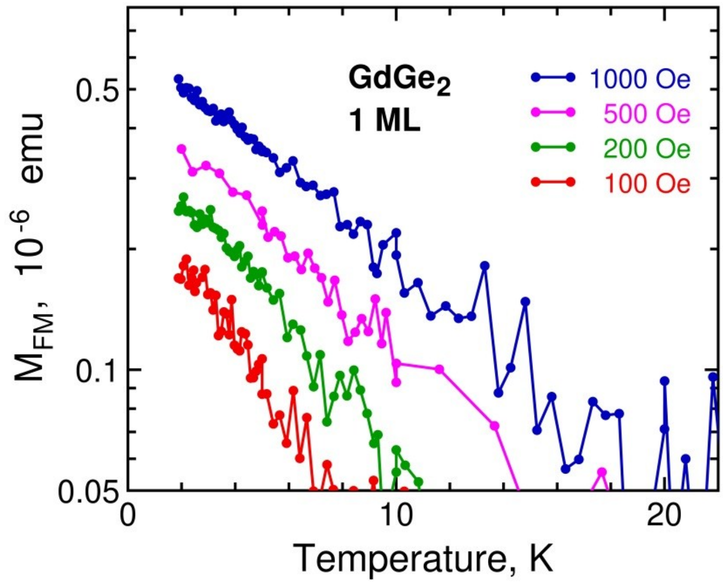

Fig. S8. Temperature dependence of the FM moment in 1 ML $GdGe_2$ measured in a number of magnetic fields along the Ge$[11\bar{2}]$ direction.

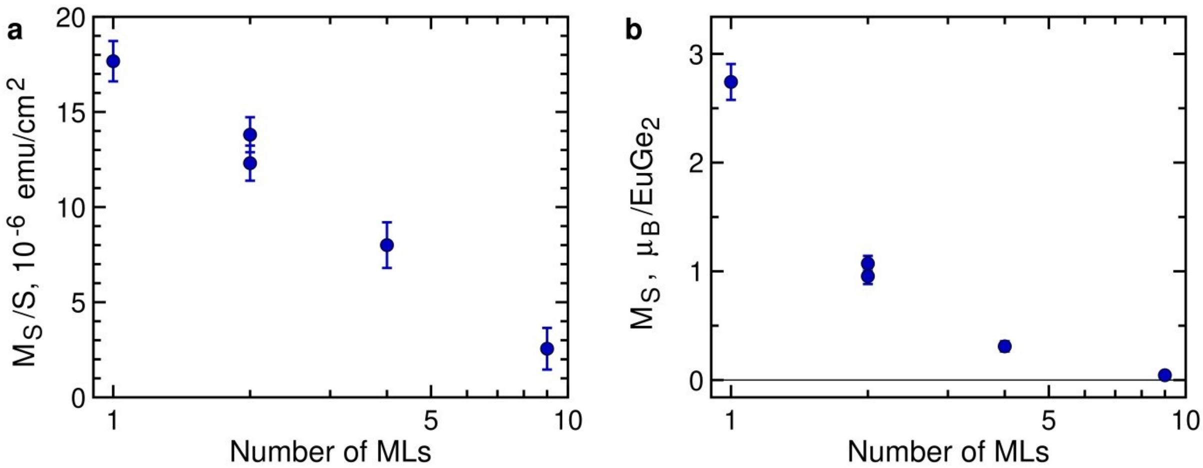

Fig. S9. Dependence of the saturation moment at 2 K in the number of MLs in $EuGe_2$. (a) Normalized to the surface area. (b) Normalized to the $EuGe_2$ formula unit.

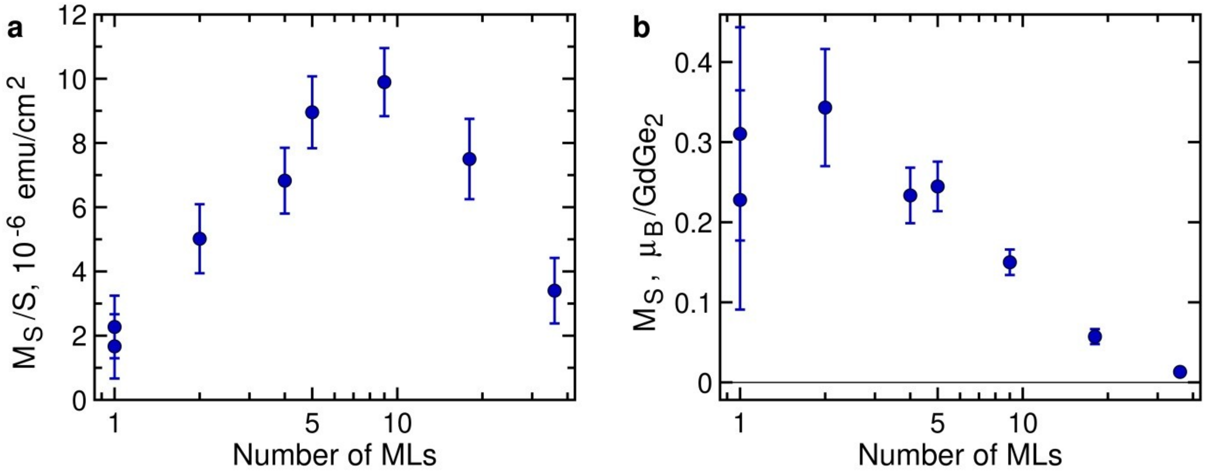

Fig. S10. Dependence of the saturation moment at 2 K in the number of MLs in $GdGe_2$. (a) Normalized to the surface area. (b) Normalized to the $GdGe_2$ formula unit.

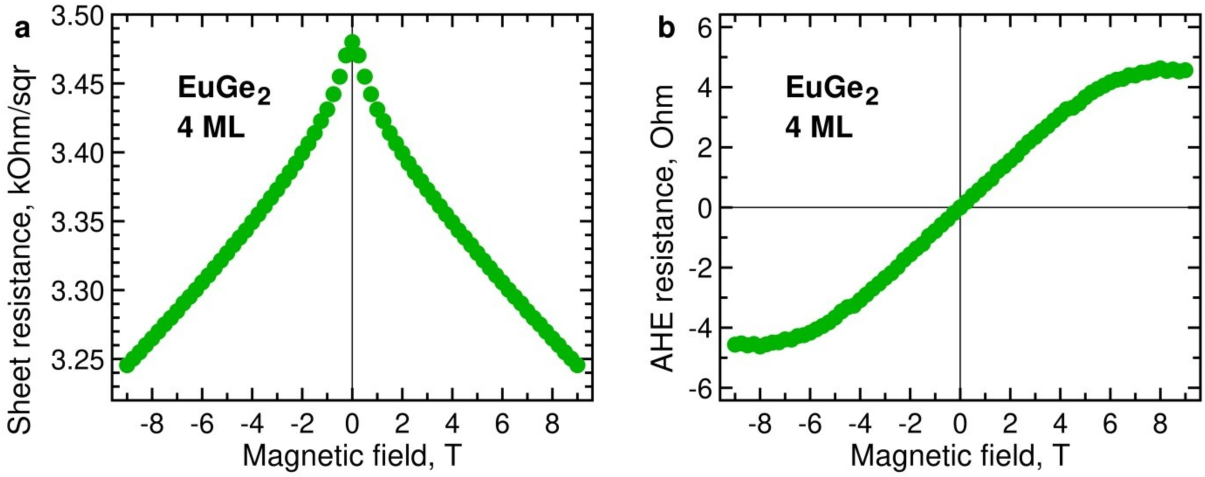

Fig. S11. Electron transport properties of 4 ML $EuGe_2$ at 2 K. (a) Magnetoresistance. (b) Anomalous Hall effect.